IJE TRANSACTIONS A: Basics Vol. 37, No. 10, (October 2024) 1882-1890

International Journal of Engineering

Journal Homepage: www.ije.ir

Numerical Investigation of Fiber Reinforced Polymer Retrofitted Short Reinforced Concrete Circular Columns under Concentric Compressive Load

A. Parghi*, M. Patel, M. H. Lunagaria

Department of Civil Engineering, Sardar Vallabhbhai National Institute of Technology, Surat, Gujarat, India

PAPER INFO

Paper history:
Received 16 December 2023
Received in revised form 10 January 2023
Accepted 23 January 2024

Keywords:
Fiber Reinforced Polymer
Circular Reinforced Concrete Columns
Retrofitting
Pre-Load
Finite Element Method

ABSTRACT

The presents study numerically investigates the fiber-reinforced polymer (FRP) retrofitted short-damaged reinforced concrete (RC) columns subjected to axial compression load. The main parameter considered to evaluate the effectiveness of FRP retrofitting on circular columns with different aspect ratios, concrete grade, and FRP material. To simulate the behaviour of a short RC column under a uniaxial compression load, a finite element model of the column was developed. The model was then modified to simulate the various level of damage to the column and the behaviour of the column under uniaxial load. The effectiveness of FRP retrofit was studied comparing the behaviour of the retrofitted column to the damaged column. For M20 concrete column retrofitted with carbon fiber reinforced polymer (CFRP) showed a higher strength (2 to 3 times) than glass fiber reinforced polymer (GFRP) retrofitted columns. For M30 concrete, the range is quite similar (1.5 – 2.3 times more). The effectiveness of both FRPs retrofitted columns increases with increasing aspect ratio from 2 and 3, but slightly decreases for an aspect ratio of 4 compared to the damaged specimen. The maximum effectiveness achieved for CFRP retrofitted columns is of 19.45% and for GFRP retrofitted column is of 10.71%, and the other grade of concrete (M30) followed a similar trend. The load-bearing capacity of columns has no significant effect by the increase in aspect ratio from 2 to 4.

***doi**: 10.5829/ije.2024.37.10a.02*

Graphical Abstract

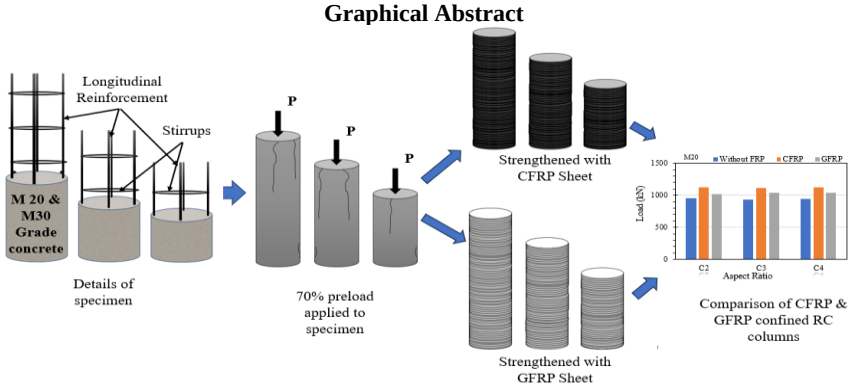

NOMENCLATURE

d_t	Tension damage variable	A_{sc}	Area of steel in compression
dc	Compression damage variable	f_y	Yield strength of steel
E1, E2	Modulus of elasticity of FRP	f_{ck}	Characteristic compressive strength of concrete
G12, G13, and G23	Shear modulus of FRP	A_c	Area of concrete
f'_c	Maximum compressive strength	**Greek Symbols**	
A_g	Gross area of RC column	μ12	Poisson's ratio of FRP

*Corresponding Author Email: amp@amd.svnit.ac.in (A. Parghi)

Please cite this article as: Parghi A, Patel M, Lunagaria MH. Numerical Investigation of Fiber Reinforced Polymer Retrofitted Short Reinforced Concrete Circular Columns under Concentric Compressive Load. International Journal of Engineering, Transactions A: Basics. 2024;37(10): 1882-90.

1. INTRODUCTION

There are numerous applications of fiber reinforced polymer (FRP) composites for strengthening of damage structural elements (1, 2). FRP composites provide many benefits, such as high strength-to-weight ratio, resistance to corrosion, and ease of installation (3-6). Yassari and Ghoulbzouri (7) numerically studied the behaviour of fiber-reinforced concrete subjected to cyclic loads using concrete damaged plasticity. They found that the concrete damaged plasticity improves the prediction of dynamic performance of fiber-reinforced concrete structures. Naji et al. (8) investigated the axial behaviour of steel fibers concrete filled steel tubes (CFST) axial load capacity, ductility, and failure modes of different sizes and shapes. They reported that adding steel fibres resulted an increase in axial load capacity, and the ductility of circular CFST columns is superior compared to square columns. Glass fiber-reinforced polymer (GFRP) is increasingly used in construction due to their unique but valuable properties compared to conventional materials. GFRPs are more prevalent, particularly for non-structural parts and secondary constructions owing to their cheaper rate (9-11). GFRP and carbon fiber-reinforced polymer (CFRP) are among the different forms of FRP utilized for the major repair and strengthening of RC components such as slabs, beams, and columns (12-15). Jabbar et al. (16) presented a comprehensive analysis using advanced numerical simulations to unravel the complexities of shear mechanisms in high-strength concrete. Methodological rigor and model validation increased the credibility of the paper and ensured the reliability of the findings. Their contribution to a comprehensive understanding of the factors influencing shear behavior is noteworthy, providing valuable insights for optimizing high-strength concrete beam design. When constructing a structure or expanding an existing one, RC columns are among the most vital structural components. A building may partially or completely collapse if the RC column fails or was not intended to withstand the appropriate load capacity. Several causes contribute to the worsening of load-displacement behavior in RC concrete columns, like preloading, design or construction flaws, alterations to the system's structure, deterioration brought on by prolonged exposure to harsh conditions or by accidental overuse, design code modifications, failure to implement a preventative maintenance plan, stress deformation due to earthquakes and exposure to extreme temperatures (17-20). Aspect ratio is also one of the influence factors for the load-carrying capacity of existing structures. The aspect ratio will also significantly affect the gaining strength of retrofitted structures (21). Till now most of the researchers have done small aspect ratios such as less than 1.5, which is suggested by the American concrete institute (ACI) and also most of the researchers performed on plain cement concrete (6). Many researchers used an aspect ratio of less than 1.5 for their study, whereas ACI (22) recommended using an aspect ratio of 1.5 due to the limited amount of experimental data. Even when the aspect ratio was more than 3, researchers found that adding transverse fiber sheets to rectangular RC columns increased their axial strength (6).

Many researchers have looked at the impact of aspect ratios on columns made of plain cement concrete, but there is relatively little information on reinforced steel concrete. For their investigations, most of the authors selected an aspect ratio of 1.5 to 2. Till now a few researchers have investigated more than 2 aspect ratios. The existing research predominantly emphasizes aspect ratio's impact on retrofitted RC column behavior, while the effect of an aspect ratio along with preloading conditions are not studied. A thorough investigation into these aspects is essential for an in-depth study of strength parameters in such columns. A comprehensive investigation into these aspects is essential for an in-depth knowledge of strength parameters in such columns. The significance of this research lies in its comprehensive numerical analysis of FRP retrofitted short RC circular columns. By systematically varying slenderness ratios, grade of concrete, and different FRP materials. It provides valuable insights into the behavior and performance of retrofitted columns under uniaxial compressive load. Details of work as flow chart are shown in Figure 1.

2. MATERIAL PROPERTIES UTILIZED IN THIS STUDY

The short RC columns are modelled using ABAQUS in this study. Concrete modelling in this software is based on the concrete damage plasticity model. The bilinear stress strain model, is used to modelled reinforcing bars. The properties of FRP materials are chosen using experimental data gathered from literatures.

2. 1. Concrete Damage Plasticity Model In this study, the concrete damaged plasticity (CDP) model of Carreira and Chu (23) is used. The CDP model is developed for applications where the concrete is exposed to different type loads and assumes scalar (isotropic) damage. The CDP model is a continuum-based concrete damage model which can be used to represent concrete and other semi-brittle materials in various constructions (shells, beams, and solids) (24). It considers cracking from tensile stress and crushing of concrete due to compressive stress as the primary failure mechanisms. Two hardening factors regulate the evolution of the yield surface under compression and tension loading (compression damage variable (dc), tension damage

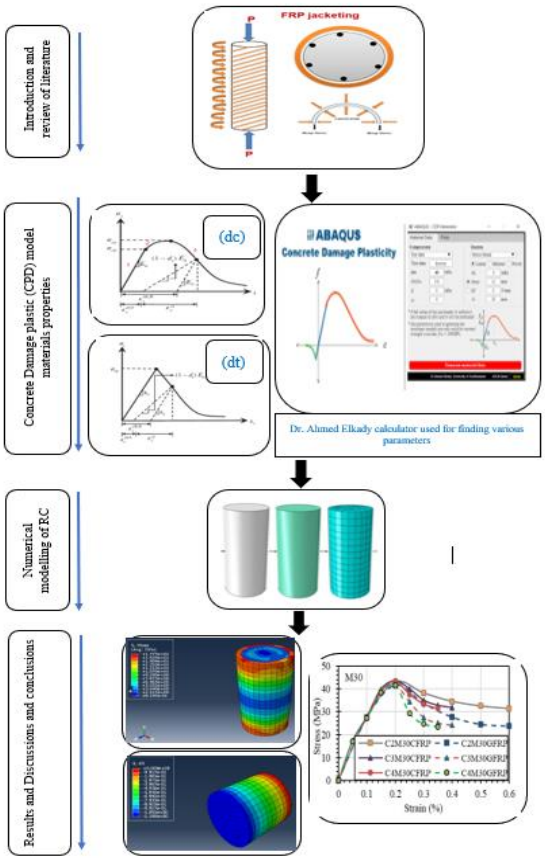

Figure 1. Flow chart of work

variable (d_t) respectively (24, 25). Elkady (26) used the MATLAB Code to create a concrete damage plasticity calculator which was based on Carreira and Chu (23) CDP model. As a consequence of this, the concrete damage plasticity calculator will produce an output that includes all of the concrete damage plasticity characteristics such as compression, tension, dc, and dt behavior for the specific grade of concrete. The CDP model is a continuum-based concrete damage model. It considers cracking from tensile stress and crushing of concrete due to compressive stress as the primary failure mechanisms. In this study, the CDP model given by Carreira and Chu (23) is used. Elkady (26) used the MatLab Coding software to create a concrete damage plasticity calculator shown in Figure 1. Table 1 lists the input parameters required by ABAQUS to run the CDP model

Compressive damage variable (d_c)

$$d_c = 1 - \frac{\sigma_c}{\sigma_{cu}}$$

Tensile damage variable (d_t)

$$d_t = 1 - \frac{\sigma_t}{\sigma_{tu}}$$

2. 2. Steel Reinforcements Steel reinforcement was employed in RC columns as main rebar's and tie bars. Steel reinforcing bar modelled in using a bilinear elastoplastic stress strain model (27).

2. 3. FRP Confined Column Figure 2 shows how FRP confines circular concrete columns (28, 29). The confining pressure of concrete is dependent on column diameter, elastic modules, and the FRP material's tensile strength. Properties of FRP materials in terms of their physical and mechanical determined by ASTM D4762-04 (30). Tables 2 and 3 summaries the parameters of the FRP material used in this investigation.

3. NUMERICAL MODELLING

In present study two different grade of concrete, two different type of FRP materials and three different aspect

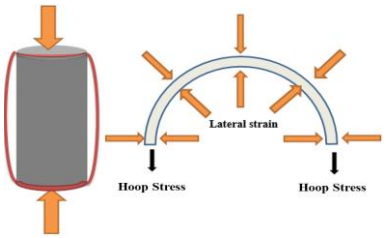

Figure 2. FRP Confinement action (29)

TABLE 1. Plasticity parameters (24, 25, 27)

Parameter	Values
Eccentricity	0.10
Dilation angle	30° – 40°
K	2/3
f_{b0}/f_{c0}	1.1667

TABLE 2. Mechanical properties of FRP (30-32)

	E_1 (GPa)	E_2 (GPa)	G_{12} (GPa)	G_{13} (GPa)	G_{23} (GPa)	μ_{12}
CFRP	126.00	11.00	6.60	6.60	4.60	0.28
GFRP	48.00	12.00	6.00	6.00	4.00	0.28

TABLE 3. Strength parameters of FRP (27, 30, 32)

	CFRP	GFRP
Longitudinal tensile strength, XT (MPa)	1950	1200
Longitudinal compressive strength, XC (MPa)	1480	800
Transverse tensile strength, YT (MPa)	48	59
Transverse compressive strength, YC (MPa)	200	128
Longitudinal shear strength (MPa)	79	25
Transverse shear strength (MPa)	79	25

ratios are used. Table 4 shows the details of the FRP composites and column dimensions. Details about reinforcement are listed in Table 5 and Schematic diagram is shown in Figure 3.

3. 1. Finite Element Modeling An RCC column consists of three components: concrete, main rebar, and tie bar. The analysis of RC short columns was performed using ABAQUS/Explicit with a period of 1 (total time step). A three-dimensional (3D) modelling space was selected, and the deformable solid extrusion type was utilized. The material was defined as elastic-isotropic, and the "CDP" material model was chosen from literature [24] with its associated characteristics as specified in Table 6. This study investigated the M20 and M30 concrete grades, which had different elastic modulus. The column element meshed with a size of 28 (system-generated value) using hexagonal elements with a sweep technique for mesh regulation. The integration modes used were explicit, linear, and C3D8R (continuum, 3-D, 8 nodes, reduced integration) for the parameter "3D stress." To model the reinforcing bars, in three-dimensional (3D) space was used using deformable wire type. The material was characterized as elastic-isotropic, and its behavior was modelled as "plasticity." To create a realistic RCC column in ABAQUS, the concrete column, main bars, and tie bars must be properly assembled. The assembly process is illustrated in Figure 4.

3. 2. Strengthening of RC Circular Columns 3D model specimen and deformable shell extrusion type were chosen to model the FRP composites. The mesh size for seeding was selected 28, and the explicit element, linear-reduced integration, and shell family with S4R node. A tie constraint was used to attach the FRP sheet to the concrete surface, allowing for load transfer between the two surfaces while also acting as an adhesive material. The FRP wrapping column in ABAQUS is depicted in Figure 5, where the green color represents the FRP sheet and the white color represents the RCC column.

3. 3. Validation of RC Column with Experimental Results Carreria and Chu (23) CDP model was used in order to create the model for the concrete column. As shown in Figure 6 the numerical result was validated with the experimental data reported by Ghali et al. (33). The variation of the experiment and numerical results was 2.02%. Maximum load carrying capacity of

TABLE 1. Short RC column details

Grade of concrete	M20, M30
Type of FRPs	CFRP, GFRP
Aspect ratios	2(200×400) 3(200×600) 4(200×800)

TABLE 5. Details of reinforcement bars

Elastic Modulus (MPa)	210000
Yield strength of main rebar (MPa)	415
Yield strength of tie rebar (MPa)	250
Area of main rebar (mm^2)	113
Area of tie bar (mm^2)	28
Poisons ratio of steel	0.30

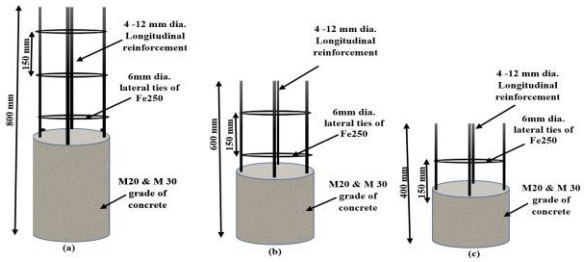

Figure 3. Schematic diagram of c/s and reinforcements a different aspect ratio of circular RC columns

TABLE 6. Concrete material properties

Mass density (ton/mm^3)	2.5×10^{-9}
Elastic modulus (MPa)	$5000\sqrt{f_{ck}}$
Poisons ratio of concrete	0.20

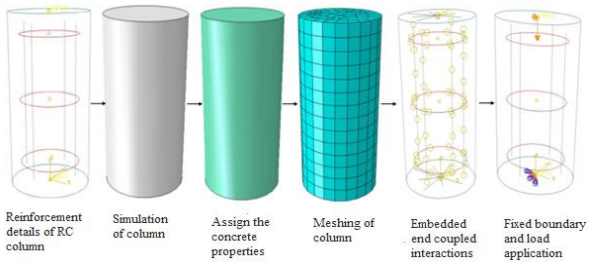

Figure 4. FEM modelling of circular columns

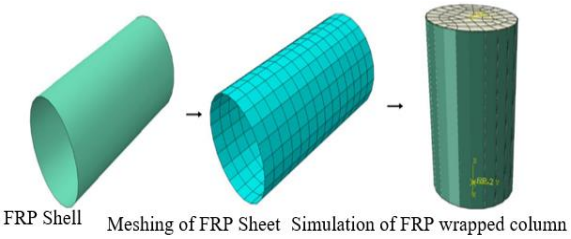

Figure 5. Strengthening of RC circular columns

unconfined RC columns was calculated using ACI318R (34) and IS 456 (35).

4. RESULT AND DISCUSSIONS

The results were recorded at each step of the process for comparison purposes. In stage-1, the axial load was applied numerically on the columns and the maximum load carrying capacity was calculated as depicted in Table 6**Error! Reference source not found.**. In stage 2, t o generate damaged in columns, The preload was applied on the columns as shown in Table 6. In stage 3, the process of repairing the damaged columns involved wrapping them with FRPs. The repaired columns were then subjected to further loading until they failed. Table 7 shows the comprehensive summary of stage 3, along with a detailed description of the data collected from ABAQUS.

4. 1. Results of Axial Load Carrying Capacity of Unconfined Columns This section of the paper describes the findings of a study conducted on the axial load-carrying capacity of an unconfined RC column. The results obtained through the numerical investigation are presented about factors such as the grade of concrete and aspect ratio.

4. 1. 1. Grade of Concrete Figure 7 depict the increase in load-carrying capacity of the various RC columns. Results showed that when the grade of concrete is upgraded from M20 to M30, there is a significant increase in the load-carrying capacity of different RC columns. For C2, it increases by 34.95%; for C3, it increases by 34.72%; and for C4, it increases by 36.59%. According to the study, increasing the concrete grade from M20 to M30 results in a significant increase in the load-carrying capacity of various RC columns. Overall, the current study adds to the existing literature on RC column load-carrying capacity and emphasizes the importance of considering concrete grade when designing for load-bearing capacity. The study's findings have implications for the design of RC structures and could be used to help develop building codes and standards.

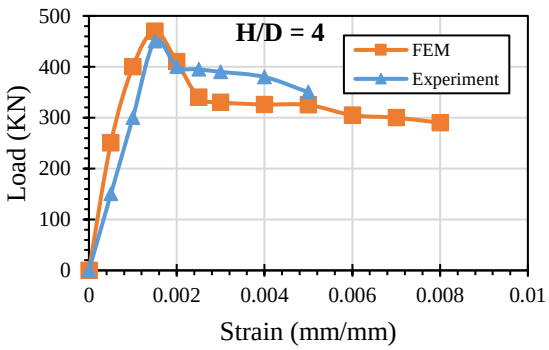

Figure 1. Stress strain relationship of circular column (Validation model)

TABLE 7. Columns maximum load carrying capacity obtained using ABAQUS

Column Specimens	Maximum stress (MPa)		Preload proposal on the columns (kN)	
	M20	M30	M20	M30
C2	30.24	40.82	665.08	897.73
C3	29.72	40.03	653.73	880.43
C4	29.90	40.87	657.68	898.80

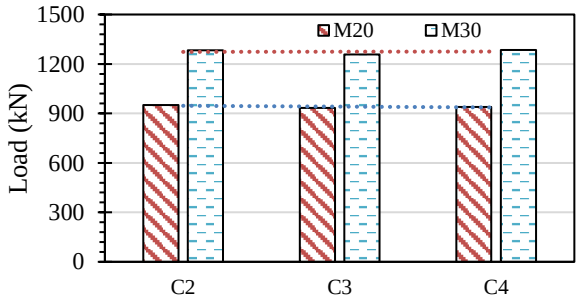

Figure 7. A comparison of the load-carrying capacity of columns of different concrete grades

4. 1. 2. Aspect Ratio As the aspect ratio of circular columns increases from 2 to 3, the load-carrying capacity of the columns decreases for M20 and M30 grades of concrete, respectively. The reduction is 1.82% for M20 and 1.98% for M30 grades of concrete. However, as the aspect ratio further increases from 3 to 4, the load-carrying capacity of the columns improves. the capacity increases by 0.64% for M20 and 2.06% for M30 grades of concrete, as shown in Figures 8 and 9.

4. 2. Results of Axial Load Carrying Capacity of Confined Columns This section describes the results of axial load-carrying capacity of CFRP and GFRP confined RC columns obtained from the numerical investigation. The analysis is based on various factors, including aspect ratio, grade of concrete and type of FRP.

4. 2. 1. Grade of Concrete The impact of aspect ratio on the load-carrying capacity for a specific grade of concrete and type of FRP is negligible. Regardless of the aspect ratio, the load-carrying capacity of columns wrapped with CFRP and GFRP sheets for M20-grade concrete is almost identical. The maximum load-carrying capacities for C2, C3, and C4 columns range from 1115 kN to 1124 kN for M20CFRP and from 1015 kN to 1040 kN for M20 GFRP. For M30CFRP and M30GFRP, the

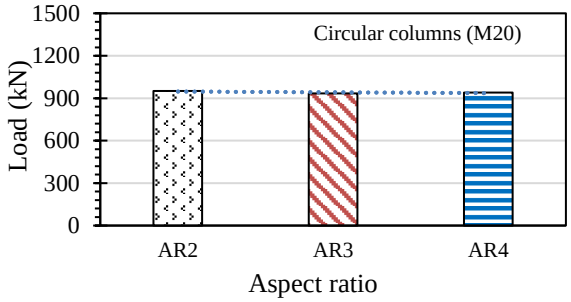

Figure 2. Load-carrying capacity comparison with different aspect ratios of M-20 columns

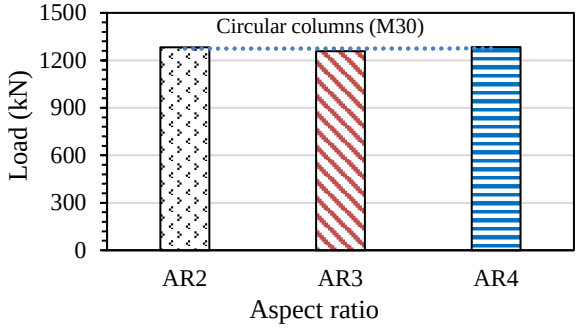

Figure 3. Load-carrying capacity comparison with different aspect ratios of M-30 columns

maximum load-carrying capacities for C2, C3, and C4 columns are between 1350 kN to 1365 kN and 1312 kN to 1325 kN, respectively. The stress-strain behavior of circular RC columns for various concrete grades is depicted in Figures 10 and 11. From the results presented in Figures 12 and 13, it can be inferred that CFRP-strengthened columns exhibit better performance than GFRP-strengthened columns. Nevertheless, it is worth noting that both types of FRP materials can enhance the load-carrying capacity of M20 and M30-grade concrete.

4. 2. 2. Aspect Ratio The load-carrying capacity of a C2 column wrapped with CFRP is 10.73% higher for M20 grade concrete and 2.89% higher for M30 grade concrete, C3 column wrapped with CFRP is 7.83% higher for M20 grade concrete and 3.01% higher for M30 grade concrete, and C4 column wrapped with CFRP is 7.69% higher for M20 grade concrete and 3.18% higher for M30 grade concrete than a column wrapped with GFRP. When the concrete grade is increased from M20 to M30, the C2 column load-carrying capacity increases by 20% for CFRP wrapped columns and by 29% for GFRP strengthened columns. C3 column load-carrying capacity increases by 22% when wrapped with CFRP and by 28% when strengthened with GFRP. The load-carrying capacity of C4 columns increases by 21% when wrapped with CFRP and by 26% when strengthened with GFRP. Figures 14, 15 and 16 illustrate stress strain curves for circular RC columns with various aspect ratios.

4. 2. 3. Type of FRP Figure 17 depicts the variation in an aspect ratio of circular columns reinforced with CFRP, which shows an increase until it reaches C3, after which it starts to decline. On the other hand, Figure 18 illustrates a circular column reinforced with GFRP, in which the aspect ratio continues to increase continuously

TABLE 8. Summary of stage 3 output data

Column specimen ID	Unconfined column maximum stress (MPa)	Confined column maximum stress (MPa)		% of increment strength carrying capacity	
		CFRP	GFRP	GFRP	CFRP
		M20			
C2	30.24	35.78	32.30	06.82	18.30
C3	29.72	35.50	32.91	10.71	19.41
C4	29.90	35.64	33.07	10.58	19.17
		M30			
C2	40.82	42.97	41.76	2.30	5.26
C3	40.03	43.44	42.17	5.34	8.50
C4	40.87	43.35	42.52	4.04	6.07

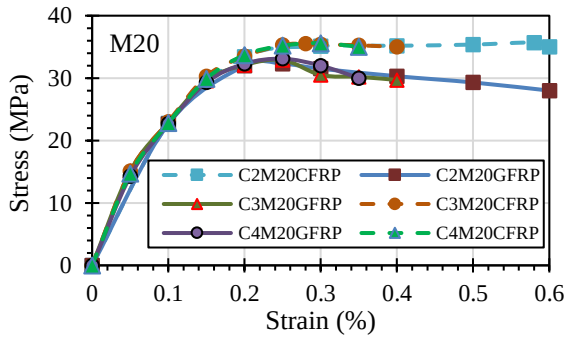

Figure 10. Stress-strain response of confined circular RC columns (M20)

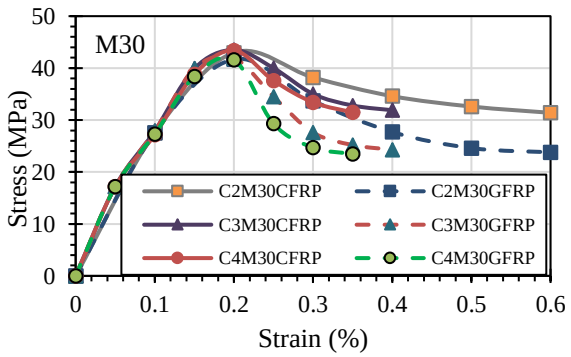

Figure 11. Stress-strain response of confined circular RC columns (M30)

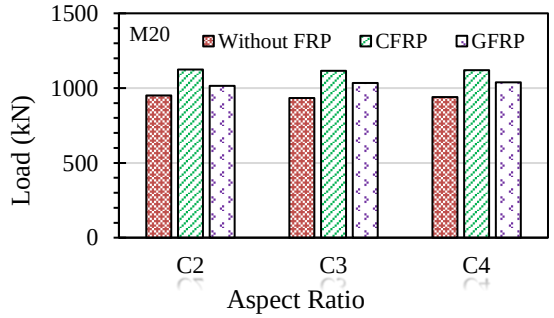

Figure 12. Load carrying capacity of confined and unconfined column specimens (M20)

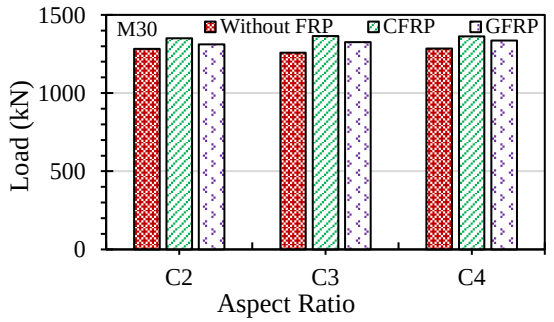

Figure 13. Load carrying capacity of confined and unconfined column specimens (M30)

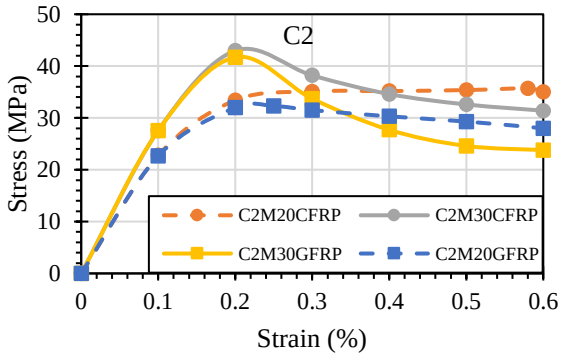

Figure 14. Stress – strain behaviour of confined C2 RC column

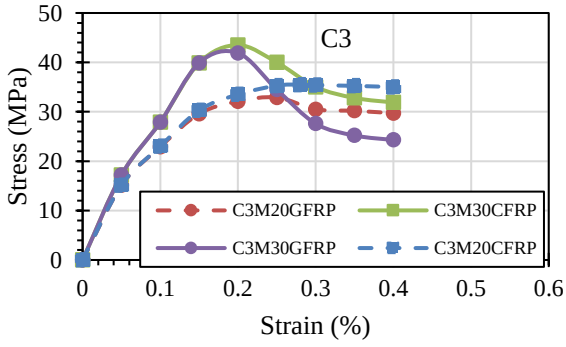

Figure 15. Stress – strain behaviour of confined C3 RC column

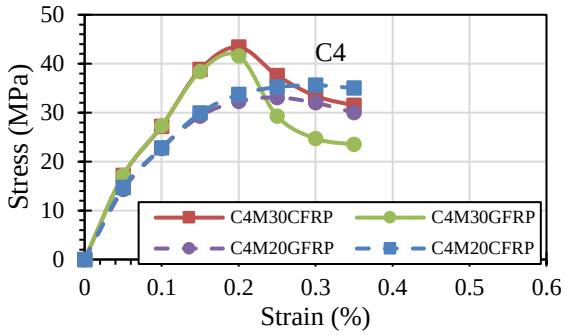

Figure 16. Stress strain behaviour of confined C4 RC column

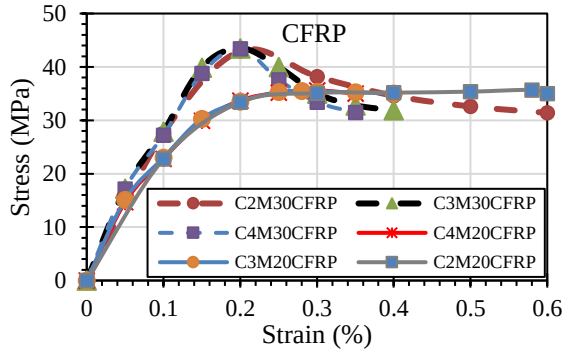

Figure 17. Stress-strain behavior of circular columns strengthened with CFRP

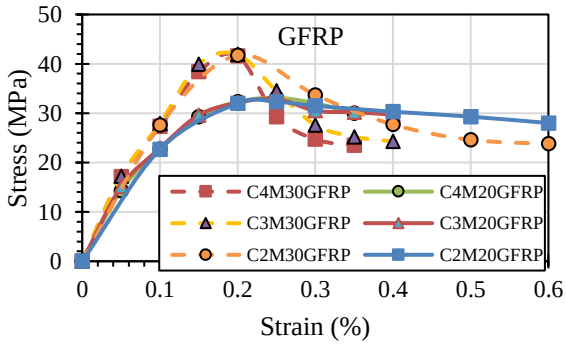

Figure 18. Stress-strain behavior of circular columns strengthened with GFRP

until it reaches C4. It can be observed that the load-carrying capacity of a column is directly proportional to the grade of concrete, as evidenced by the performance of the CFRP-strengthened column. FRP-strengthened columns' load-bearing capacity depends on concrete strength, with higher grades carrying more.

5. CONCLUSIONS

The present research focused on the numerical investigation on the effects of grade of concrete, aspect

ratio (2, 4 and 6) of the column, and type of FRP used for column wrapping. Based on the numerical investigation, the following conclusions are drawn:

- Increasing the concrete grade from M20 to M30, 38% in the maximum load capacity of both square and circular columns increased. These findings suggest that the load-bearing capacity of concrete is directly correlated with its grade, irrespective of The numerical results obtained from ABAQUS reveals that the load-carrying capacity of columns is underestimated by IS 456 and ACI 318R standards, as these standards are designed with the factor of safety.
- When the aspect ratio increases from AR2 to AR4, the load-carrying capacity reaches about 1120 kN (M20), and 1340 kN (M30). 19.17% for (CFRP-M20) and 10.58% for (GFRP-M20), 6.07% for (CFRP-M30) and 4.04% for (GFRP-M30).
- The aspect ratio has minimal impact on the load capacity of both confined and unconfined circular columns, which remains consistent across various aspect ratios.
- CFRP wrapping columns have superior axial loadcolumn geometry.
- -Carrying capacity performance when compared to GFRP confinement columns.
- When the grade of concrete is upgraded from M20 to M30, circular columns reinforced with CFRP show greater improvement in strength compared to those reinforced with GFRP.
- The study showed the importance of the grade of concrete and aspect ratio in the behaviour of confined RC columns, which should be considered when designing these structures.

6. REFERENCES

1. Ashrafi H, Bazli M, Najafabadi EP, Oskouei AV. The effect of mechanical and thermal properties of FRP bars on their tensile performance under elevated temperatures. Construction and building materials. 2017;157:1001-10. https://doi.org/10.1016/j.conbuildmat.2017.09.160
2. Ashrafi H, Bazli M, Vatani Oskouei A, Bazli L. Effect of sequential exposure to UV radiation and water vapor condensation and extreme temperatures on the mechanical properties of GFRP bars. Journal of composites for construction. 2018;22(1):04017047. https://doi.org/10.1061/(asce)cc.1943-5614.0000828
3. Chowdhury EU, Bisby LA, Green MF, Kodur VK. Investigation of insulated FRP-wrapped reinforced concrete columns in fire. Fire safety journal. 2007;42(6-7):452-60. https://doi.org/10.1016/j.firesaf.2006.10.007
4. Kodur V, Yu B. Evaluating the fire response of concrete beams strengthened with near-surface-mounted FRP reinforcement. Journal of Composites for Construction. 2013;17(4):517-29. https://doi.org/10.1061/(asce)cc.1943-5614.0000348
5. Kodur V, Ahmed A. Numerical model for tracing the response of FRP-strengthened RC beams exposed to fire. Journal of Composites for Construction. 2010;14(6):730-42. https://doi.org/10.1061/(asce)cc.1943-5614.0000129
6. Li X, Lu J, Ding D-D, Wang W. Axial strength of FRP-confined rectangular RC columns with different cross-sectional aspect ratios. Magazine of Concrete Research. 2017;69(19):1011-26. https://doi.org/10.1680/jmacr.17.00036
7. El Yassari S, El Ghoulbzouri A. Numerical simulation of fiber-reinforced concrete under cyclic loading using extended finite element method and concrete damaged plasticity. International Journal of Engineering, Transactions A: Basics. 2023;36(10):1815-26. https://doi.org/10.5829/ije.2023.36.10a.08
8. Naji A, Al-Jelawy H, Hassoon A, Al-Rumaithi A. Axial behavior of concrete filled-steel tube columns reinforced with steel fibers. International Journal of Engineering, Transactions B: Applications. 2022;35(9):1682-9. https://doi.org/10.5829/ije.2022.35.09c.02
9. Goldston M, Remennikov A, Sheikh MN. Experimental investigation of the behaviour of concrete beams reinforced with GFRP bars under static and impact loading. Engineering Structures. 2016;113:220-32. https://doi.org/10.1016/j.engstruct.2016.01.044
10. Oskouei AV, Bazli M, Ashrafi H, Imani M. Flexural and web crippling properties of GFRP pultruded profiles subjected to wetting and drying cycles in different sea water conditions. Polymer Testing. 2018;69:417-30. https://doi.org/10.1016/j.polymertesting.2018.05.038
11. Bazli M, Jafari A, Ashrafi H, Zhao X-L, Bai Y, Raman RS. Effects of UV radiation, moisture and elevated temperature on mechanical properties of GFRP pultruded profiles. Construction and Building Materials. 2020;231:117137. https://doi.org/10.1016/j.conbuildmat.2019.117137
12. Ma G, Yan L, Shen W, Zhu D, Huang L, Kasal B. Effects of water, alkali solution and temperature ageing on water absorption, morphology and mechanical properties of natural FRP composites: Plant-based jute vs. mineral-based basalt. Composites Part B: Engineering. 2018;153:398-412. https://doi.org/10.1016/j.compositesb.2018.09.015
13. Kodur V, Bhatt P. A numerical approach for modeling response of fiber reinforced polymer strengthened concrete slabs exposed to fire. Composite Structures. 2018;187:226-40. https://doi.org/10.1016/j.compstruct.2017.12.051
14. Bazli M, Ashrafi H, Oskouei AV. Experiments and probabilistic models of bond strength between GFRP bar and different types of concrete under aggressive environments. Construction and Building Materials. 2017;148:429-43. https://doi.org/10.1016/j.conbuildmat.2017.05.046
15. Hawileh RA, Abu-Obeidah A, Abdalla JA, Al-Tamimi A. Temperature effect on the mechanical properties of carbon, glass and carbon–glass FRP laminates. Construction and building materials. 2015;75:342-8. https://doi.org/10.1016/j.conbuildmat.2014.11.020
16. Jabbar AM, Mohammed DH, Hasan QA. A numerical study to investigate shear behavior of high-strength concrete beams externally retrofitted with carbon fiber reinforced polymer sheets. International Journal of Engineering, Transactions B: Applications. 2023;36(11):2112-23. https://doi.org/10.5829/IJE.2023.36.11B.15
17. Biswas R, Iwanami M, Chijiwa N, Nakayama K. Structural assessment of the coupled influence of corrosion damage and seismic force on the cyclic behaviour of RC columns. Construction and Building Materials. 2021;304:124706. https://doi.org/10.1016/j.conbuildmat.2021.124706

18. Özkılıç YO, Aksoylu C, Gemi L, Arslan MH, editors. Behavior of CFRP-strengthened RC beams with circular web openings in shear zones: Numerical study. Structures; 2022: Elsevier.
19. Li L, Wang H, Wu J, Du X, Zhang X, Yao Y. Experimental and numerical investigation on impact dynamic performance of steel fiber reinforced concrete beams at elevated temperatures. Journal of Building Engineering. 2022;47:103841. https://doi.org/10.1016/j.jobe.2021.103841
20. Hu J, Zhang S, Chen E, Li W. A review on corrosion detection and protection of existing reinforced concrete (RC) structures. Construction and Building Materials. 2022;325:126718. https://doi.org/10.1016/j.conbuildmat.2022.126718
21. Farghal OA. Structural performance of axially loaded FRP-confined rectangular concrete columns as affected by cross-section aspect ratio. HBRC journal. 2018;14(3):264-71. https://doi.org/10.1016/j.hbrcj.2016.11.002
22. Soudki K, Alkhrdaji T, editors. Guide for the design and construction of externally bonded FRP systems for strengthening concrete structures (ACI 440.2 R-02). Structures Congress 2005: Metropolis and Beyond; 2005.
23. Carreira DJ, Chu K-H, editors. Stress-strain relationship for plain concrete in compression. Journal proceedings; 1985.
24. ABAQUS A. 6.14, Abaqus 6.14 Anal. User's Guid. 2014;14.
25. Minh H-L, Khatir S, Wahab MA, Cuong-Le T. A concrete damage plasticity model for predicting the effects of compressive high-strength concrete under static and dynamic loads. Journal of Building Engineering. 2021;44:103239. https://doi.org/10.1016/j.jobe.2021.103239
26. Elkady A. Abaqus Tutorial: Defining Concrete Damage Plasticity Model+ Failure and Element Deletion. YouTube, YouTube. 2021. https://doi.org/10.5281/zenodo.7755926
27. Hafezolghorani M, Hejazi F, Vaghei R, Jaafar MSB, Karimzade K. Simplified damage plasticity model for concrete. Structural engineering international. 2017;27(1):68-78. https://doi.org/10.2749/101686616X1081
28. Raza A, Ahmad A. Numerical investigation of load-carrying capacity of GFRP-reinforced rectangular concrete members using CDP model in ABAQUS. Advances in Civil Engineering. 2019;2019. https://doi.org/10.1155/2019/1745341
29. Parghi A, Alam MS. Seismic behavior of deficient reinforced concrete bridge piers confined with FRP–A fractional factorial analysis. Engineering Structures. 2016;126:531-46. https://doi.org/10.1016/j.engstruct.2016.08.011
30. Benzaid R, Mesbah HA. Circular and square concrete columns externally confined by CFRP composite: experimental investigation and effective strength models. Fiber reinforced polymers–The technology applied for concrete repair. 2013:167-201. https://doi.org/10.5772/51589
31. Cepero-Mejías F, Curiel-Sosa J, Zhang C, Phadnis V. Effect of cutter geometry on machining induced damage in orthogonal cutting of UD polymer composites: FE study. Composite Structures. 2019;214:439-50. https://doi.org/10.1016/j.compstruct.2019.02.012
32. Soldani X, Santiuste C, Miguélez MH. Machining FEM model of long fiber composites for aeronautical components. 2009. https://doi.org/10.1016/j.compstruct.2009.09.021
33. Ghali K, Rizkalla S, Kassem M, Fawzy T, Mahmoud M, editors. FRP-confined circular columns under small eccentric loading. 5th Alexandria International Conference on Structural and Geotechnical Engineering; 2003.
34. Institute AC, editor Building Code Requirements for Structural Concrete (ACI 318-08) and Commentary: An ACI Standard2008: American Concrete Institute.
35. Syal I, Goel A. Reinforced Concrete Structure: S. Chand Publishing; 2008.

Persian Abstract

چکیده

مطالعه حاضر به طور عددی ستون‌های بتن مسلح آسیب‌دیده کوتاه (RC)مقاوم‌سازی شده با پلیمر تقویت‌شده با الیاف (FRP)را که تحت بار فشاری محوری قرار دارند، بررسی می‌کند. پارامتر اصلی در نظر گرفته شده برای ارزیابی اثربخشی مقاوم سازی FRP بر روی ستون های دایره ای با نسبت های مختلف، عیار بتن و مواد FRP.برای شبیه سازی رفتار یک ستون RC کوتاه تحت یک بار فشرده سازی تک محوری، یک مدل المان محدود از ستون توسعه داده شد. سپس مدل برای شبیه سازی سطوح مختلف آسیب به ستون و رفتار ستون تحت بار تک محوری اصلاح شد. اثربخشی مقاوم سازی FRP با مقایسه رفتار ستون مقاوم سازی شده با ستون آسیب دیده مورد مطالعه قرار گرفت. برای ستون بتنی M20 مقاوم‌سازی شده با پلیمر تقویت‌شده با فیبر کربن (CFRP)استحکام بالاتری (۲ تا ۳ برابر) نسبت به ستون‌های تقویت‌شده پلیمری تقویت‌شده با الیاف شیشه (GFRP)نشان داد. برای بتن M30، دامنه کاملاً مشابه است (۱.۵ – ۲.۳ برابر بیشتر). اثربخشی هر دو ستون مقاوم سازی شده با FRP با افزایش نسبت ابعاد از ۲ و ۳ افزایش می یابد، اما برای نسبت ابعاد ٤ نسبت به نمونه آسیب دیده اندکی کاهش می یابد. حداکثر اثربخشی به‌دست‌آمده برای ستون‌های مقاوم‌سازی‌شده با CFRP 19.45 درصد و برای ستون‌های مقاوم‌سازی‌شده GFRP 10.71 درصد است و گرید دیگر بتن (M30)روند مشابهی را دنبال کرد. ظرفیت باربری ستون ها با افزایش نسبت تصویر از ۲ به ٤ تأثیر معنی داری ندارد.